

# Text-to-TrajVis: Enabling Trajectory Data Visualizations from Natural Language Questions

Tian Bai<sup>1</sup>, Huiyan Ying<sup>1</sup>, Kailong Suo<sup>1</sup>, Junqiu Wei<sup>2</sup>, Tao Fan<sup>3</sup>, Yuanfeng Song<sup>3</sup>

<sup>1</sup>Jilin University, <sup>2</sup>Macau University of Science and Technology, <sup>3</sup>WeBank AI

## Abstract

This paper introduces the **Text-to-TrajVis** task, which aims to transform natural language questions into trajectory data visualizations, facilitating the development of natural language interfaces for trajectory visualization systems. As this is a novel task, there is currently no relevant dataset available in the community. To address this gap, we first devised a new visualization language called Trajectory Visualization Language (TVL) to facilitate querying trajectory data and generating visualizations. Building on this foundation, we further proposed a dataset construction method that integrates Large Language Models (LLMs) with human efforts to create high-quality data. Specifically, we first generate TVLs using a comprehensive and systematic process, and then label each TVL with corresponding natural language questions using LLMs. This process results in the creation of the first large-scale Text-to-TrajVis dataset, named **TrajVL**, which contains 18,140 (*question, TVL*) pairs. Based on this dataset, we systematically evaluated the performance of multiple LLMs (GPT, Qwen, Llama, etc.) on this task. The experimental results demonstrate that this task is both feasible and highly challenging and merits further exploration within the research community.

## 1 Introduction

The surge in human-generated trajectory data, especially from vehicles, such as the GeoLife+ (Amiri et al., 2024b), T-Drive (Yuan et al., 2010), and WorldTrace (Zhu et al., 2024b) datasets, has provided researchers with a wealth of spatio-temporal information. Visualization techniques are becoming increasingly important for understanding trajectory patterns and for in-depth analysis in areas such as human mobility pattern analysis (Toch et al., 2019; Zhu et al., 2024a), infectious disease transmission modeling (Amiri et al., 2024a; Kohn et al., 2023) and animal migration tracking (Konzack

et al., 2019). However, existing query and visualization methods often require specialized knowledge, preventing non-expert users from effectively deriving insights from trajectory data.

Natural Language to Visualization (NL2VIS) technology focuses on the automated translation of natural language queries into visualization specifications (Song et al., 2024, 2022). This technology empowers non-expert users to readily visualize trajectory data, offering novel avenues for addressing the aforementioned challenges. To this end, we introduce the Text-to-TrajVis task. In this framework, users pose trajectory data visualization requests using natural language, and the Text-to-TrajVis technology parses these queries to identify key information, including area, time, and relevant query parameters. Subsequently, the natural language query is transformed into Trajectory Visualization Language (TVL), which is then employed to automatically generate a visualization program that renders the queried data as a map or chart. For example, a natural language query that requests trajectory visualization is transformed into a map-based visualization, as illustrated in Figure 1 (see A.1 for the transformation process of other visualization charts).

Large language models have shown remarkable generalization ability in the field of natural language processing. In addition to making breakthroughs in traditional tasks such as text generation and Q&A systems, LLMs have enabled the construction of knowledge indexing libraries through Retrieval-Augmented Generation (RAG), significantly improving the accuracy and domain adaptability of the generation tasks. A typical LLM-based workflow for generating trajectory data visualizations involves assembling natural language queries and corresponding examples into prompts, and then prompting the LLM to generate a corresponding TVL. However, to the best of our knowledge, a dedicated NL2VIS dataset for trajectory

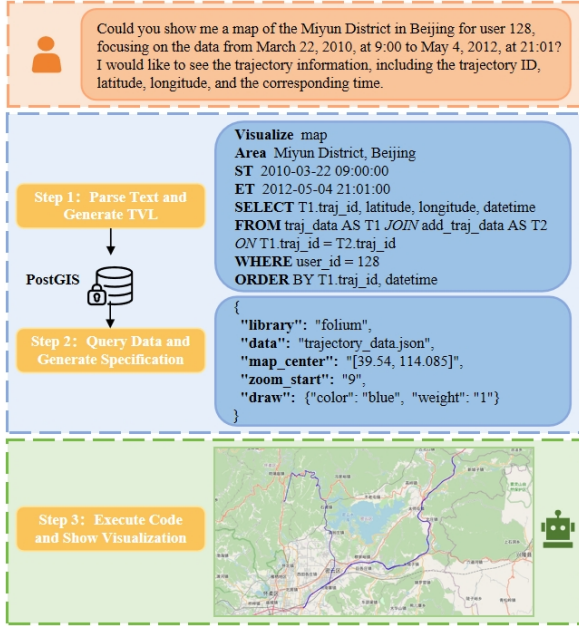


Figure 1: The process of transforming natural language question into visualization.

visualization, suitable for benchmarking LLMs, remains unavailable.

To address this gap, we introduce TrajVL, the first benchmark dataset specifically designed for the Text-to-TrajVis domain. We constructed a generalized template and a systematic methodology for generating TVL. This methodology contains two key stages: First, representative TVLs were generated as seed dataset by incorporating geographical area and temporal information into the template. Second, we developed a tree structure based on query constraints, where each leaf node represents a specific constraint or a combination thereof. Then, constraints added to the TVLs to generate a richer dataset. Recognizing that manual verification requires less time and effort than manual natural language question writing, we used LLMs to generate multiple, distinct natural language questions for each TVL. Each generated natural language question was manually reviewed to ensure it accurately and comprehensively described the corresponding TVL. Our benchmark dataset contains 6,988 TVLs and 18,140 (*question, TVL*) pairs.

We evaluated the proposed TrajVL dataset using various LLMs (e.g., GPT, Qwen, Llama, and DeepSeek). Surprisingly, the best-performing model achieved 74.61% TVL accuracy in normal scenarios. However, in the scenarios that test the model’s spatio-temporal reasoning ability, the best-performing model only achieved about 57.88% and

68.63% TVL accuracy in few-shot scenarios. The results of the evaluation indicate that the challenge of the Text-to-TrajVis task deserves further exploration by the research community.

In summary, the main contributions of this paper are as follows:

- We introduce the Text-to-TrajVis task and propose a dataset construction method that combines LLMs with human efforts.
- We introduce TrajVL, the first benchmark dataset designed specifically for the Text-to-TrajVis domain, containing 18,140 (*question, TVL*) pairs.
- We evaluated various LLM-based methods (GPT, Qwen, Llama, etc.) on the dataset to establish the baseline performance and characterize the key properties of the proposed Text-to-TrajVis task.

## 2 Related Work

### 2.1 Trajectory Data Storage

Existing geospatial database systems, such as GeoMesa (Hughes et al., 2015), ArcGIS (Law and Collins, 2019), PostGIS (Obe and Hsu, 2021), and Google BigQuery (Mucchetti, 2020), can be extended to manage trajectory data. PostGIS, in particular, offers a comprehensive set of functions and indexes for storing and querying trajectory data (Zhang and Yi, 2010). It also supports spatial indexing methods, such as R-trees, which significantly accelerate trajectory queries. The integration of PostGIS with MobilityDB (Zimányi et al., 2020) extends its ability to handle large-scale trajectory data. Furthermore, PostGIS provides a rich collection of spatial functions (Obe and Hsu, 2021) for calculating distances, areas, and lengths, as well as for determining spatial relationships.

### 2.2 Trajectory Data Visualization

Existing trajectory data visualization methods exhibit considerable diversity. One of the most fundamental approaches involves plotting trajectories as line segments on a map (He et al., 2019), which offers a straightforward representation of movement paths. In the trajectory data visualization domain, a variety of specialized languages have been developed for describing, querying, and manipulating trajectory data. GeoJSON (Butler et al., 2016), an open standard JSON-based format, is widely used

<b>VISUALIZE</b>	::= map   bar   line   pie   scatter   heat map   contour plot
<b>AREA</b>	area $\in$ ({geographical_name})
<b>ST</b>	st $\in$ ({null, timestamp})
<b>ET</b>	et $\in$ ({null, timestamp}), et > st (if st, et $\neq$ null)
<b>SELECT</b>	C   CC   CCC   C...C (C ::= column)
<b>FROM</b>	T
<b>TRANSFORM</b>	::= avg   count   sum   group by   binning   max   min
<b>ORDER BY</b>	::= asc C   desc C

Figure 2: The structure of Trajectory Visualization Language.

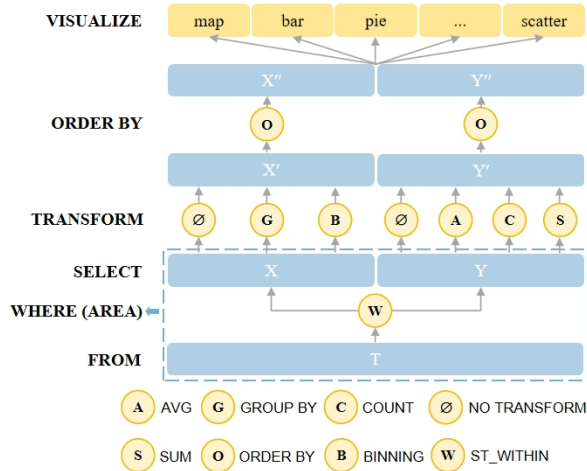


Figure 3: The visualization workflow for Trajectory Visualization Language.

for representing various geospatial data structures. Programming languages and their corresponding libraries, such as Python and JavaScript, offer more flexible programming interfaces for visualizing trajectory data. For instance, the Folium (Suma et al., 2024) library in Python offers the functionality of constructing interactive web maps using Leaflet (Crickard III, 2014). Libraries such as GeoPandas (Jordahl et al., 2021), Shapely (Gillies et al., 2023), and Cartopy (Elson et al., 2022) provide functions for processing and visualizing trajectory data.

### 2.3 Text-to-Visualization

The field of NL2VIS has garnered increasing attention with advancements in visualization technology (Cox et al., 2001; Gao et al., 2015; Liu et al., 2021; Narechania et al., 2020; Luo et al., 2021b,a). Many studies employ deep neural networks to learn the mapping between NLQs and visualization specifications (Dibia and Demiralp, 2019; Song et al., 2022; Liu et al., 2023; Li et al., 2023b; Xiang et al., 2023). To facilitate text-to-visualization development, researchers have also introduced corresponding datasets. Luo et al. proposed the NVBench dataset (Luo et al., 2021a) as a benchmark for NL2VIS research. Song et

Table 1: TrajVL dataset statistics

Vis-Type	TVL	(TVL, NLQ)
Map	4,873	12,377
Bar Chart	788	2,256
Line Chart	727	1,997
Pie Chart	600	1,510
Total	6,988	18,140

al. introduced Dial-NVBench (Song et al., 2024), a benchmark dataset designed for interactive visualization research. Currently, LLM-based approaches have become the dominant paradigm in NL2VIS research (Gan et al., 2021; Dong et al., 2023; Li et al., 2023a; Pourreza and Rafiei, 2023; Gao et al., 2023), significantly enhancing task performance through the synergistic interplay of semantic parsing and code generation. Pre-trained LLMs have also been increasingly applied to these tasks. For instance, Chat2vis (Maddigan and Susnjak, 2023) utilizes a bimodal prompting strategy involving “natural language query + tabular element”, prompting engineering-driven LLMs to generate visualization code. Tian’s team proposed a task decoupling strategy that focuses on visualization task-oriented fine-tuning of LLMs, fine-tuning the FLAN-T5 model (Chung et al., 2024) to ChartGPT (Tian et al., 2024) in stages.

While significant progress has been made in NL2VIS research, trajectory visualization remains largely unexplored. Our work is the first systematic effort to address this research gap. We introduce a specialized dataset (i.e., TrajVis), evaluation metrics, and comprehensive evaluations tailored for this task. Experimental and human evaluations validate the utility of this dataset, and we anticipate that it will facilitate future research in trajectory-aware visual analytics and advance other domain-specific work in NL2VIS applications.

## 3 TrajVL Datasets

### 3.1 Data Collection & Preparation

Trajectory data used for constructing TrajVL are sourced from the GPS trajectory dataset released by the GeoLife project (Zheng et al., 2011). This dataset, which was collected from 182 users from April 2007 to August 2012, contains 17,621 trajectories, each represented by a series of timestamped points. Each point contains latitude, longitude, and altitude information. The dataset also includes a

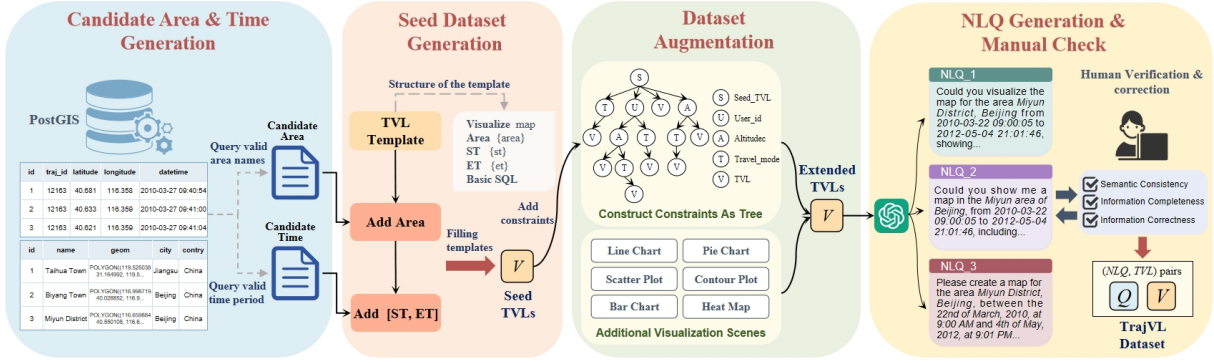


Figure 4: The pipeline of constructing the TrajVL dataset. The construction of TrajVL involves four main steps: (i) collecting all geographic areas and their associated time ranges from the trajectory database as candidates; (ii) generating representative TVLs as seed data by integrating geographic areas and temporal information into the template; (iii) enriching the dataset by expanding TVLs using a tree-structured augmentation approach and by adding other visualization scenes; and (iv) generating multiple types of natural language questions via LLMs, followed by manual validation.

label file for each user, which indicates travel mode labels. User movement trajectories are mainly distributed across more than 30 cities in China, with the majority of the data originating from Beijing.

To obtain information about the administrative boundaries of Chinese provinces at various levels, we utilized the Chinese area boundary data files provided by OpenStreetMap (Haklay and Weber, 2008). This area boundary information was subsequently imported and stored within the PostGIS database.

**Trajectory Visualization Language** We designed a template for generating TVL queries. This template encompasses visualization types, geographical areas, temporal information, and fundamental SQL structures. The *VISUALIZE* component specifies the desired visualization type and transforms the queried data into a visualization query expressed in a specific language (e.g., Python, Vega-Lite). For trajectory data, spatio-temporal information is crucial and can be utilized to impose conditional constraints on the queried data. The spatial dimension enables the specification of geographical entity names via the *AREA* parameter. The temporal dimension employs a dual-anchor constraint mechanism, where start time and end time define a closed interval  $[ST, ET]$ . Within the SQL structure, the *TRANSFORM* operator integrates trajectory analysis-specific functions, including temporal binning, spatial aggregation (*group by*), and statistical computation (*avg/count/sum/max/min*), to construct a transformation pipeline  $T(x) \rightarrow x'$ . The *ORDER BY* extension facilitates a sorting strategy based on the

transformed variables (e.g., binning interval, aggregated values), and specifies the sorting direction via *ASC* or *DESC*. Figure 2 defines the structure of the TVL.

The workflow of TVL embeds spatio-temporal semantics into structured queries through a formal constraint mechanism. This mechanism automatically translates the *AREA* and  $[ST, ET]$  parameters into SQL *WHERE* clause constraints during the syntactic parsing phase. For spatial constraints, the expression "*ST\_Within(geometry\_column, spatial\_filter)*" is dynamically generated. Here, the *spatial\_filter* is parsed as a geofence in WKT format using a library of predefined names. For temporal constraints, the filter condition "*date-time\_column BETWEEN ST AND ET*" is generated (see A.3 for details). The workflow of TVL ensures seamless integration of spatio-temporal constraints with standard SQL syntax, as illustrated in Figure 3.

### 3.2 Dataset Construction

**Seed Dataset Generation** Since the trajectory data is stored in a database, we first collected all geographical areas within the trajectory data to validate areas before incorporating them into the template. These collected areas served as a candidate selections. Next, we extracted the earliest and latest timestamps of trajectories within each area to define temporal ranges. From each range, we selected 3-5 time intervals to form temporal candidates. Finally, representative TVL queries were then generated by selecting geographical areas and time intervals from the candidates.

**Dataset Augmentation** We designed a tree struc-

Dataset	Size	Query Language	Output Type	Task Type	Construction	Multi-Type NL Question
Spider	10,181	SQL	Data	NL2SQL	Manual	✗
nvBench	25,750	VQL	Vis	NL2VIS	Manual+Synthesis	✗
GeoQuery	877	SQL	Geo-data	NL2GIS	Manual	✗
NLMAP V2	28,609	MRL	Geo-data	NL2GIS	Manual	✗
OverpassQL	8,352	OverpassQL	Geo-data	NL2OSM	Manual	✗
TrajVL	18,140	<b>TVL</b>	<b>Geo-vis</b>	<b>NL2TrajVis</b>	<b>Manual+LLM</b>	✓

Table 2: Comparison of TrajVL with other existing Text-to-Query datasets. Notice that Multi-Type NL Question refers to whether each Query supports multiple types of NL questions, not just the entire dataset.

ture with additional constraints for trajectory data querying, aiming to enrich and diversify TVL. Besides latitude and longitude in the basic table, the database has auxiliary tables storing extra trajectory attributes. We extracted and organized attributes like user ID, travel mode, and altitude to form query constraints, using them as the foundation for the tree structure where leaf nodes represent specific or combined constraints. By embedding these nodes into the SQL query structure of TVL, we generated a more comprehensive dataset, and the constraints can be optimized as more attributes are added to meet diverse user needs.

We found that complementary trajectory features, such as travel mode and altitude, can be utilized to construct novel visual query paradigms. Therefore, variations in travel mode and altitude within trajectories were selected as core analytical dimensions and integrated with spatio-temporal constraints to generate TVL. This methodology was employed to generate queries for three common visualization types: pie charts, line charts, and bar charts to expand the dataset. This dataset can be extended to support other visualization types, including scatter plots and heat maps. Complete implementation details are provided in A.2.

**Natural Language Questions Generation** Considering the labor-intensive and time-consuming process of manual generation of natural language questions, we opted to use LLMs for this task. Considering the paramount importance of area and time information within trajectory data, we sequentially provided three distinct prompts to the LLM to generate diversified descriptions of each TVL, primarily differing in the articulation of geographical areas and times. This approach facilitated the generation of 2-3 corresponding natural language queries for each TVL query. Detailed prompts and

generated samples are provided in A.4.

**Manual Check** We used a manual evaluation method to assess the quality of the NLQs generated by LLM based on TVL, mainly examining quality indicators in three dimensions: semantic consistency, information completeness and information correctness. The manual assessment results show that the following quality issues exist in the samples: 11.96% of the samples present semantic redundancy, 13.1% of the samples have missing information problems, and 8.4% of the samples contain information errors. Specifically, semantic redundancy refers to the fact that the generated NLQ contains information content that is not related to TVL. Information missing is manifested as the NLQ failing to cover all the necessary fields in the TVL. Information error is manifested by the NLQ’s description of key information such as time, area, and SQL being inconsistent with the TVL. To address the above three types of data quality problems, we designed a differentiated prompt strategy (see Appendix A.5 for details) to guide LLMs to make NLQs corrections. The corrected NLQs underwent a second round of manual validation focused on verifying the accuracy of the corrections. Through the iterative correction and validation process, we finally achieved a comprehensive optimization of data quality, ensuring the accuracy and reliability of the generated data. The dataset generation workflow is illustrated in Figure 4.

### 3.3 Dataset Analysis

The dataset contains four prevalent visualization types, including maps, bar charts, line charts, and pie charts. It contains a total of 6,988 visualization instances. For each visualization, TrajVL contains one to several natural language questions, contain-

ing a total of 18,140 (*question, TVL*) pairs (Table 1). The percentage of maps in the dataset is 69.7%, because map is the most common chart type in trajectory data visualization. In addition, visual queries also include those like “Display the percentage of travel by each mode in Beijing over the past year” and “Display the change in altitude of the user’s trajectory over a period of time”, etc. Therefore, we expanded the number of three types of visualization charts: bar charts, line charts, and pie charts. These expansions accounted for 11.3%, 10.4%, and 8.6% respectively of the dataset. Our dataset covers 9 provinces and includes a total of 638 areas, most of which are located in Hebei and Beijing.

### 3.4 Comparison to Other Datasets

Since we are the first to provide a dataset for the Text-to-TrajVis task, we conducted comparative analyses with the dataset of related tasks (see Table 2). Geoquery (Zelle and Mooney, 1996) is a small dataset with 877 instances. The natural language queries in this dataset are hand-written to simulate geographic information queries that a user might make, and it queries 937 different geographic facts about the United States. NLMAP V2 (Lawrence and Riezler, 2018) provided queries about OpenStreetMap paired with natural language input. However, these queries are written in a restricted query language called Machine Readable Language (MRL), which is an abstraction of the OverpassQL. OverpassQL (Staniek et al., 2024) contains queries in the well-established OverpassQL language with additional features for accessing and retrieving geographic information from the OpenStreetMap database. Compared to our dataset, these datasets focus primarily on querying geographic data rather than data visualization. The Spider (Yu et al., 2018) dataset was designed for the Text-to-SQL task. The NvBench (Luo et al., 2021a) dataset was constructed based on Spider and is designed to provide high-quality benchmark data for the NL2VIS task. However, it does not include visualization of trajectory data. In contrast to NvBench, our dataset is designed to support trajectory data querying and visualization, with a construction process that combines LLM and manual annotation. LLM can generate large volumes of data rapidly, and manual annotation ensures data quality.

## 4 Experimental Setup

**Dataset Splitting** We partitioned the dataset into a training set containing 5,012 instances and a test set containing 1,973 instances. The test set was constructed through stratified sampling to ensure representative coverage of diverse query intents and to mitigate bias in the evaluation of specific patterns. Following the methodology described in Section 3.2, we generated either one (when temporal information was absent) or two different natural language questions for each TVL in the Normal test set. As a result, three distinct test sets were generated: Normal test set, Area test set and Time test set. The Area test set and the Time test set were designed to evaluate the accuracy of the LLM in generating TVLs when processing complex spatio-temporal descriptions.

**Models** To systematically evaluate the performance of diverse LLMs in the TVL generation task, we selected four representative models, which encompass both proprietary and open-source architectures. The selected models include GPT-4 (Achiam et al., 2023), Llama-3 (Grattafiori et al., 2024), Qwen (Yang et al., 2024), and DeepSeek-LLM (Bi et al., 2024). The experiments adopted a few-shot prompting paradigm. Each input prompt contains a system task instruction, an annotated demonstration example of translating a natural language query to TVL, and the target query for parsing. Details of these models are provided in Appendix B.1.

**Metrics** To evaluate the performance of LLMs in generating TVL, we adopted *Vis Accuracy*, *Axis Accuracy*, and *Data Accuracy*, metrics commonly employed in text-to-vis tasks (Luo et al., 2021a). Given the critical role of spatio-temporal information in trajectory data, the SQL query for retrieving such data is synthesized from the area, time, and the fundamental SQL query structure. Consequently, within the Data Accuracy assessment, we employ Area Accuracy and Time Accuracy to evaluate the precision of LLM-generated spatio-temporal information. The detailed definition of these metrics can be found in Appendix B.2.

## 5 Results and Discussion

This section presents a comprehensive evaluation of the performance of LLMs on the dataset. Experiments revealed that Qwen2.5-7b and GPT-4o-mini achieved peak performance with a 6-shot prompting configuration, while Deepseek-llm-7b

Test Set	Model	Vis.Acc	Axis.Acc	Data.Acc			
				Area	Time	SQL	TVL
Normal	DeepSeek-llm-7b	99.95	86.47	82.51	81.96	40.14	35.94
	Llama3-8b	99.70	89.20	86.92	94.88	57.27	53.07
	Qwen2.5-7b	99.95	98.78	98.43	99.75	64.93	64.06
	GPT-4o-mini	99.85	98.94	98.78	99.19	65.64	<b>64.67</b>
Area	DeepSeek-llm-7b	100.0	72.93	61.94	84.64	37.56	24.33
	Llama3-8b	99.70	75.92	64.88	93.87	53.22	37.61
	Qwen2.5-7b	100.0	83.53	74.96	99.65	62.75	47.24
	GPT-4o-mini	99.75	82.11	72.58	98.88	64.62	<b>47.74</b>
Time	DeepSeek-llm-7b	100.0	84.24	79.02	75.06	37.91	27.88
	Llama3-8b	99.49	88.29	84.79	89.31	50.13	41.92
	Qwen2.5-7b	100.0	97.31	95.84	93.72	62.70	55.90
	GPT-4o-mini	99.95	97.62	96.00	94.68	63.30	<b>56.66</b>

Table 3: Comparison of performance for each LLM on TrajVL.

Test Set	Model	Vis.Acc	Axis.Acc	Data.Acc			
				Area	Time	SQL	TVL
Normal	DeepSeek-llm-7b	98.88	86.16	81.60	96.40	65.89	58.19
	Llama3-8b	99.95	96.05	94.58	97.77	74.76	71.31
	Qwen2.5-7b	100.0	98.68	98.07	99.95	76.03	74.56
	GPT-4o-mini	99.95	99.19	98.58	99.95	75.47	<b>74.61</b>
Area	DeepSeek-llm-7b	99.59	83.83	74.71	96.25	64.93	49.27
	Llama3-8b	99.70	78.97	69.42	96.69	70.07	52.87
	Qwen2.5-7b	99.70	85.96	78.36	99.65	73.29	<b>57.88</b>
	GPT-4o-mini	99.65	84.79	76.08	99.70	74.56	57.32
Time	DeepSeek-llm-7b	99.95	90.22	86.67	87.33	66.65	55.30
	Llama3-8b	100.0	94.98	93.22	93.66	73.20	64.38
	Qwen2.5-7b	99.95	97.87	96.15	95.39	74.76	67.66
	GPT-4o-mini	100.0	97.87	96.30	96.30	75.06	<b>68.63</b>

Table 4: Comparison of performance for each RAG-enhanced LLM on TrajVL.

and Llama3-8b achieved peak performance with a 4-shot and 5-shot prompting configuration, respectively (see C.1 for details). Accordingly, Table 3 presents the performance of LLMs on the three test sets, and Table 4 details the results of RAG-enhanced LLMs.

**Performance of LLMs on Test Sets** Table 3 presents the TVL accuracy results for various models across different test sets. GPT-4o-mini achieved a TVL accuracy of 64.67% on the Normal test set. However, its performance decreased to 47.74% and 56.66% on the Area and Time test sets, respectively. This suggests that GPT-4o-mini is notably sensitive to complex area descriptions, while tem-

poral constraints have a comparatively smaller impact. DeepSeek-llm-7b, Llama3-8b, and Qwen2.5-7b had lower TVL accuracy in both the Area and Time test sets than in the Normal test set. This indicates that the performance of these models is significantly hindered by both complex regional and temporal descriptions. Qwen2.5-7b’s performance was second only to that of the GPT-4o-mini when it came to handling spatial and temporal complexity, but further improvements are needed.

The Vis.Acc approached 100% for most models, indicating robust performance in visual type recognition. Regarding Axis.Acc, all models exhibited significantly higher performance on the Normal

and Time test sets than on the Area test set. This is due to the need for centering the map visualization on a specific area, establishing strong dependencies between the visual component and the spatial area. This strong dependency means complex area descriptions may also impair the accurate identification of visualization components. Similarly, Data.Acc showed a significant decrease in performance when processing the Area and Time test sets, suggesting that complex spatio-temporal descriptions pose a challenge to the models. The SQL accuracy remained relatively stable across most models, even in the presence of complex spatio-temporal descriptions. This stability stems from the experimental design, where the SQL evaluation metrics focused on base SQL queries. Area and time information was integrated into the base SQL after TVL generation, thus mitigating the direct impact of spatio-temporal complexity on SQL accuracy during the experimental validation process (as detailed in Section 3.1). However, DeepSeek-llm-7b, Llama3-8b, and Qwen2.5-7b demonstrated a decrease in SQL accuracy. This decline is likely due to difficulties encountered by these models in parsing NLQs containing complex time and area descriptions. These parsing challenges resulted in a reduction of the number of correctly formatted TVL outputs, thus affecting SQL extraction. Conversely, GPT-4o-mini exhibited more stable performance, resulting in fewer fluctuation in SQL accuracy.

**Performance of RAG-enhanced LLMs on Test Sets** As presented in Table 4, all RAG-enhanced models surpassed their corresponding base models in both TVL and SQL accuracy. The models’ TVL and SQL generation results across the three test sets were consistent with the trends observed in Table 3. However, despite the RAG enhancement, complex spatial and temporal descriptions remained challenging for the models. In the Area test set, Axis.Acc and Area.Acc generally declined across all models compared to the Normal test set, with GPT-4o-mini and Qwen2.5-7b showing the most significant decrease. While Qwen2.5-7b and GPT-4o-mini show the most significant downward trend, their overall performance is still better than DeepSeek-llm-7b and Llama3-8b, which indicates their superior ability in extracting core semantic elements and processing complex spatial descriptions. Similarly, in the Time test set, model performance on temporal descriptions generally decreased, but not as much as in the Area test set. The consistently high performance of GPT-4o-mini

and Qwen2.5-7b in the Time test set further demonstrates their superior capability to handle complex temporal descriptions. Despite the high Time accuracy achieved by GPT-4o-mini and Qwen2.5-7b, temporal complexity still affects the accuracy of TVL generation.

Overall, GPT-4o-mini achieved the highest TVL accuracy across Normal test set and Time test set, demonstrating particular robustness in complex scenarios. The RAG-enhanced Qwen2.5-7b model followed closely, achieved the highest TVL accuracy in the Area test set. DeepSeek-llm-7b showed poorer performance with lower TVL accuracy than Llama3-8b. Although the RAG technique significantly improved the performance of LLMs in TVL generation tasks, especially for basic scenarios, its effectiveness remained limited for complex spatio-temporal semantics.

## 6 Conclusion

This paper introduces TrajVL, the first benchmark dataset for the Text-to-TrajVis task. We designed TVL, a novel visualization language, to facilitate trajectory data querying and visualization generation. A dataset construction process combining LLM capabilities with manual refinement was developed, ensuring high-quality NLQ and TVL queries. Subsequently, we evaluated multiple LLMs on TrajVL, revealing challenges in processing spatio-temporal information for Text-to-TrajVis. Experimental results demonstrate that while Retrieval-Augmented Generation (RAG) improves LLM performance, significant limitations persist in handling complex spatio-temporal information.

Future work will investigate enhancing LLMs’ performance in processing Text-to-TrajVis tasks. Specifically, we will focus on improving the performance of end-to-end TVL generation from natural language queries with complex spatio-temporal information. This work contributes to the ongoing advancement of the TrajVis field and inspire further research innovations.

## 7 Limitations

We have proposed a dataset generation framework that combines LLM with human intervention, and constructed the first large-scale Text-to-TrajVis benchmark dataset, named TrajVL, to address the lack of benchmark datasets in this field. However, the trajectory data utilized to construct the

dataset mainly came from a single data source (GeoLife project dataset). Although the dataset was effectively expanded through a systematic approach, the insufficient amount of additional information on the trajectory data limited the complexity of the constraint tree. In addition, the Area Test and Time Test cannot comprehensively cover all real-world situations with complex descriptions of spatio-temporal information. Therefore, future research should extend the dataset generation framework to other trajectory datasets for generating more general TVLs. The TrajVL dataset can be further extended by integrating richer additional information about trajectories and constructing more complex constraint trees. More diverse and complex spatio-temporal descriptions of real-world trajectories should also be incorporated into the NLQ generation process to enhance the challenge of the dataset.

## References

- Josh Achiam, Steven Adler, Sandhini Agarwal, Lama Ahmad, Ilge Akkaya, Florencia Leoni Aleman, Diogo Almeida, Janko Altenschmidt, Sam Altman, Shyamal Anadkat, et al. 2023. Gpt-4 technical report. *arXiv preprint arXiv:2303.08774*.
- Hossein Amiri, Ruochen Kong, and Andreas Züfle. 2024a. Urban anomalies: A simulated human mobility dataset with injected anomalies. In *Proceedings of the 1st ACM SIGSPATIAL International Workshop on Geospatial Anomaly Detection*, pages 1–11.
- Hossein Amiri, Richard Yang, and Andreas Züfle. 2024b. Geolife+: Large-scale simulated trajectory datasets calibrated to the geolife dataset. In *Proceedings of the 7th ACM SIGSPATIAL International Workshop on GeoSpatial Simulation*, pages 25–28.
- Xiao Bi, Deli Chen, Guanting Chen, Shanhuang Chen, Damai Dai, Chengqi Deng, Honghui Ding, Kai Dong, Qiusi Du, Zhe Fu, et al. 2024. Deepseek llm: Scaling open-source language models with longtermism. *arXiv preprint arXiv:2401.02954*.
- Howard Butler, Martin Daly, Allan Doyle, Sean Gillies, Stefan Hagen, and Tim Schaub. 2016. The geojson format. Technical report.
- Hyung Won Chung, Le Hou, Shayne Longpre, Barret Zoph, Yi Tay, William Fedus, Yunxuan Li, Xuezhi Wang, Mostafa Dehghani, Siddhartha Brahma, et al. 2024. Scaling instruction-finetuned language models. *Journal of Machine Learning Research*, 25(70):1–53.
- Kenneth Cox, Rebecca E Grinter, Stacie L Hibino, Lalita Jategaonkar Jagadeesan, and David Mantilla. 2001. A multi-modal natural language interface to an information visualization environment. *International Journal of Speech Technology*, 4:297–314.
- Paul Crickard III. 2014. *Leaflet. js essentials*. Packt Publishing Ltd.
- Victor Dibia and Çağatay Demiralp. 2019. Data2vis: Automatic generation of data visualizations using sequence-to-sequence recurrent neural networks. *IEEE computer graphics and applications*, 39(5):33–46.
- Xuemei Dong, Chao Zhang, Yuhang Ge, Yuren Mao, Yunjun Gao, Jinshu Lin, Dongfang Lou, et al. 2023. C3: Zero-shot text-to-sql with chatgpt. *arXiv preprint arXiv:2307.07306*.
- Phil Elson, Elliott Sales De Andrade, Greg Lucas, Ryan May, Richard Hattersley, Ed Campbell, Andrew Dawson, Stephane Raynaud, Bill Little, Alan D Snow, et al. 2022. Scitools/cartopy: v0. 21.0. *Zenodo*.
- Yujian Gan, Xinyun Chen, Jinxia Xie, Matthew Purver, John R Woodward, John Drake, and Qiaofu Zhang. 2021. Natural sql: Making sql easier to infer from natural language specifications. *arXiv preprint arXiv:2109.05153*.
- Dawei Gao, Haibin Wang, Yaliang Li, Xiuyu Sun, Yichen Qian, Bolin Ding, and Jingren Zhou. 2023. Text-to-sql empowered by large language models: A benchmark evaluation. *arXiv preprint arXiv:2308.15363*.
- Tong Gao, Mira Dontcheva, Eytan Adar, Zhicheng Liu, and Karrie G Karahalios. 2015. Datatone: Managing ambiguity in natural language interfaces for data visualization. In *Proceedings of the 28th annual acm symposium on user interface software & technology*, pages 489–500.
- Sean Gillies, Casper van der Wel, Joris Van den Bossche, Mike W Taves, Joshua Arnott, Brendan C Ward, et al. 2023. Shapely. *Zenodo*.
- Aaron Grattafiori, Abhimanyu Dubey, Abhinav Jauhri, Abhinav Pandey, Abhishek Kadian, Ahmad Al-Dahle, Aiesha Letman, Akhil Mathur, Alan Schelten, Alex Vaughan, et al. 2024. The llama 3 herd of models. *arXiv e-prints*, pages arXiv–2407.
- Mordechai Haklay and Patrick Weber. 2008. Openstreetmap: User-generated street maps. *IEEE Pervasive computing*, 7(4):12–18.
- Jing He, Haonan Chen, Yijin Chen, Xinming Tang, and Yebin Zou. 2019. Diverse visualization techniques and methods of moving-object-trajectory data: A review. *ISPRS International Journal of Geo-Information*, 8(2):63.
- James N Hughes, Andrew Annex, Christopher N Eichelberger, Anthony Fox, Andrew Hulbert, and Michael Ronquest. 2015. Geomesa: a distributed architecture for spatio-temporal fusion. In *Geospatial informatics, fusion, and motion video analytics V*, volume 9473, pages 128–140. SPIE.

- Kelsey Jordahl, Joris Van den Bossche, Jacob Wasserman, James McBride, Jeffrey Gerard, Jeff Tratner, Matthew Perry, and Carson Farmer. 2021. geopandas/geopandas: v0. 5.0. *Zenodo*.
- Will Kohn, Hossein Amiri, and Andreas Züfle. 2023. Epipol: An epidemiological patterns of life simulation (demonstration paper). In *Proceedings of the 4th ACM SIGSPATIAL International Workshop on Spatial Computing for Epidemiology*, pages 13–16.
- Maximilian Konzack, Pieter Gijsbers, Ferry Timmers, Emiel van Loon, Michel A Westenberg, and Kevin Buchin. 2019. Visual exploration of migration patterns in gull data. *Information Visualization*, 18(1):138–152.
- Michael Law and Amy Collins. 2019. Getting to know arcgis pro. (*No Title*).
- Carolin Lawrence and Stefan Riezler. 2018. Improving a neural semantic parser by counterfactual learning from human bandit feedback. In *Proceedings of the 56th Annual Meeting of the Association for Computational Linguistics (Volume 1: Long Papers)*, pages 1820–1830.
- Haoyang Li, Jing Zhang, Cuiping Li, and Hong Chen. 2023a. Resdsq: Decoupling schema linking and skeleton parsing for text-to-sql. In *Proceedings of the AAAI Conference on Artificial Intelligence*, volume 37, pages 13067–13075.
- Jinyang Li, Binyuan Hui, Reynold Cheng, Bowen Qin, Chenhao Ma, Nan Huo, Fei Huang, Wenyu Du, Luo Si, and Yongbin Li. 2023b. Graphix-t5: Mixing pre-trained transformers with graph-aware layers for text-to-sql parsing. In *Proceedings of the AAAI conference on artificial intelligence*, volume 37, pages 13076–13084.
- Can Liu, Yun Han, Ruike Jiang, and Xiaoru Yuan. 2021. Advisor: Automatic visualization answer for natural-language question on tabular data. In *2021 IEEE 14th Pacific Visualization Symposium (PacificVis)*, pages 11–20. IEEE.
- Hu Liu, Yuliang Shi, Jianlin Zhang, Xinjun Wang, Hui Li, and Fanyu Kong. 2023. Multi-hop relational graph attention network for text-to-sql parsing. In *2023 International Joint Conference on Neural Networks (IJCNN)*, pages 1–8. IEEE.
- Yuyu Luo, Nan Tang, Guoliang Li, Chengliang Chai, Wenbo Li, and Xuedi Qin. 2021a. Synthesizing natural language to visualization (nl2vis) benchmarks from nl2sql benchmarks. In *Proceedings of the 2021 International Conference on Management of Data*, pages 1235–1247.
- Yuyu Luo, Nan Tang, Guoliang Li, Jiawei Tang, Chengliang Chai, and Xuedi Qin. 2021b. Natural language to visualization by neural machine translation. *IEEE Transactions on Visualization and Computer Graphics*, 28(1):217–226.
- Paula Maddigan and Teo Susnjak. 2023. Chat2vis: Generating data visualizations via natural language using chatgpt, codex and gpt-3 large language models. *Ieee Access*, 11:45181–45193.
- Mark Mucchetti. 2020. *BigQuery for Data Warehousing*. Springer.
- Arpit Narechania, Arjun Srinivasan, and John Stasko. 2020. N14dv: A toolkit for generating analytic specifications for data visualization from natural language queries. *IEEE Transactions on Visualization and Computer Graphics*, 27(2):369–379.
- Regina Obe and Leo Hsu. 2021. *PostGIS in action*. Simon and Schuster.
- Mohammadreza Pourreza and Davood Rafiei. 2023. Din-sql: Decomposed in-context learning of text-to-sql with self-correction. *Advances in Neural Information Processing Systems*, 36:36339–36348.
- Yuanfeng Song, Xuefang Zhao, and Raymond Chi-Wing Wong. 2024. Marrying dialogue systems with data visualization: Interactive data visualization generation from natural language conversations. In *Proceedings of the 30th ACM SIGKDD Conference on Knowledge Discovery and Data Mining*, pages 2733–2744.
- Yuanfeng Song, Xuefang Zhao, Raymond Chi-Wing Wong, and Di Jiang. 2022. Rgvisnet: A hybrid retrieval-generation neural framework towards automatic data visualization generation. In *Proceedings of the 28th ACM SIGKDD Conference on Knowledge Discovery and Data Mining*, pages 1646–1655.
- Michael Staniek, Raphael Schumann, Maike Züfle, and Stefan Riezler. 2024. Text-to-overpassql: A natural language interface for complex geodata querying of openstreetmap. *Transactions of the Association for Computational Linguistics*, 12:562–575.
- KG Suma, Gurram Sunitha, J Avanija, Mohammad Gouse Galety, and Chinthapatla Pranay Varna. 2024. Geospatial data visualization with folium. In *Geospatial Application Development Using Python Programming*, pages 187–208. IGI global.
- Yuan Tian, Weiwei Cui, Dazhen Deng, Xinjing Yi, Yurun Yang, Haidong Zhang, and Yingcai Wu. 2024. Chartgpt: Leveraging llms to generate charts from abstract natural language. *IEEE Transactions on Visualization and Computer Graphics*.
- Eran Toch, Boaz Lerner, Eyal Ben-Zion, and Irad Ben-Gal. 2019. Analyzing large-scale human mobility data: a survey of machine learning methods and applications. *Knowledge and Information Systems*, 58:501–523.
- Yanzheng Xiang, Qian-Wen Zhang, Xu Zhang, Zejie Liu, Yunbo Cao, and Deyu Zhou. 2023. G3r: A graph-guided generate-and-rerank framework for complex and cross-domain text-to-sql generation. In *Findings of the Association for Computational Linguistics: ACL 2023*, pages 338–352.

- An Yang, Baosong Yang, Beichen Zhang, Binyuan Hui, Bo Zheng, Bowen Yu, Chengyuan Li, Dayiheng Liu, Fei Huang, Haoran Wei, et al. 2024. Qwen2. 5 technical report. *arXiv preprint arXiv:2412.15115*.
- Tao Yu, Rui Zhang, Kai Yang, Michihiro Yasunaga, Dongxu Wang, Zifan Li, James Ma, Irene Li, Qingning Yao, Shanelle Roman, et al. 2018. Spider: A large-scale human-labeled dataset for complex and cross-domain semantic parsing and text-to-sql task. In *Proceedings of the 2018 Conference on Empirical Methods in Natural Language Processing*, pages 3911–3921.
- Jing Yuan, Yu Zheng, Chengyang Zhang, Wenlei Xie, Xing Xie, Guangzhong Sun, and Yan Huang. 2010. [T-drive: driving directions based on taxi trajectories](#). In *ACM SIGSPATIAL International Workshop on Advances in Geographic Information Systems*.
- John M Zelle and Raymond J Mooney. 1996. Learning to parse database queries using inductive logic programming. In *Proceedings of the national conference on artificial intelligence*, pages 1050–1055.
- Lijing Zhang and Jing Yi. 2010. Management methods of spatial data based on postgis. In *2010 Second Pacific-Asia Conference on Circuits, Communications and System*, volume 1, pages 410–413. IEEE.
- Yu Zheng, Hao Fu, Xing Xie, Wei Ying Ma, and Qunnan Li. 2011. Geolife gps trajectory dataset - user guide.
- Feng Zhu, Chen Chang, Zhiheng Li, Boqi Li, and Li Li. 2024a. [A generic optimization-based enhancement method for trajectory data: Two plus one](#). *Accident; analysis and prevention*, 200:107532.
- Yuanshao Zhu, James Jian Qiao Yu, Xiangyu Zhao, Xuetao Wei, and Yuxuan Liang. 2024b. [Unitraj: Learning a universal trajectory foundation model from billion-scale worldwide traces](#). *ArXiv*, abs/2411.03859.
- Esteban Zimányi, Mahmoud Sakr, and Arthur Lesuisse. 2020. Mobilitydb: A mobility database based on postgresql and postgis. *ACM Transactions on Database Systems (TODS)*, 45(4):1–42.

## A More Implementation Details

### A.1 Generating visualization specifications based on TVL

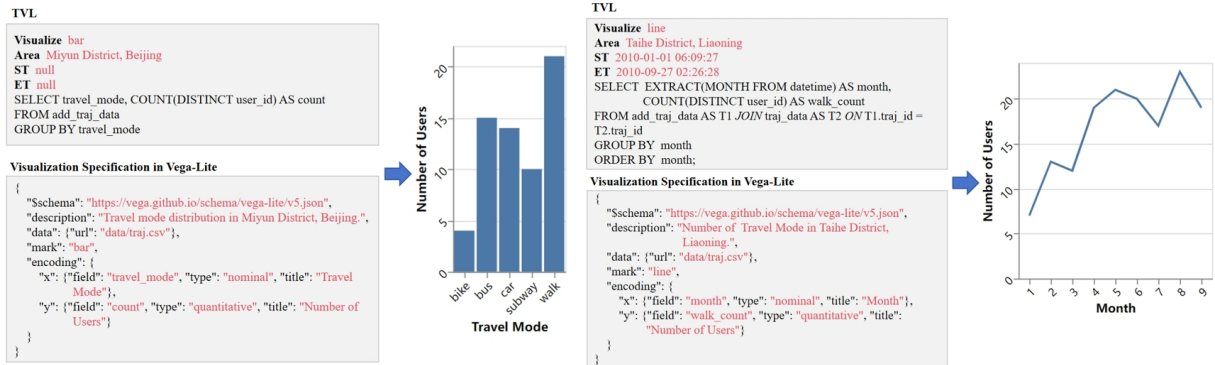


Figure 5: Examples of the visualization specification in Vega-Lite, and its corresponding visualization.

The proposed Text-to-TrajVis system implements an automatic mapping mechanism from natural language queries to TVLs. As shown in Figure 5, the generated TVL contains three core components: (i) Visualization type statement: specifying the chart presentation form; (ii) Spatio-temporal constraint parameters: constructing geo-spatio-temporal filtering conditions; and (iii) SQL query statement: realizing semantic fusion of trajectory attributes and spatio-temporal coordinates through multi-table association. For standardized chart types (bar charts, line charts, etc.), the system adopts Vega-Lite, a declarative visualization specification framework, which precisely defines the visual coding rules through JSON syntax. The proposed architecture ensures end-to-end interpretability from semantic parsing to visual presentation through formal language transformation mechanisms.

### A.2 Construction Details for Additional Types of Visualization

<p><b>Template of travel_mode:</b></p> <pre>Visualize ::= bar   line   pie   scatter   heat map   contour plot Area area ∈ ({null, geographical_name}) ST st ∈ ({null, timestamp}) ET et ∈ ({null, timestamp}, et &gt; st (if st, et ≠ null)) SELECT travel_mode, COUNT(DISTINCT user_id) AS count FROM add_traj_data AS T1 JOIN traj_data AS T2 ON T1.traj_id = T2.traj_id GROUP BY travel_mode;</pre>	<p><b>Template of altitude:</b></p> <pre>Visualize ::= bar   line   pie   scatter   heat map   contour plot Area area ∈ ({null, geographical_name}) ST st ∈ ({null, timestamp}) ET et ∈ ({null, timestamp}, et &gt; st (if st, et ≠ null)) SELECT datetime, altitude FROM traj_data AS T1 JOIN add_traj_data AS T2 ON T1.traj_id = T2.traj_id ORDER BY datetime;</pre>
---	--

Figure 6: Templates for extended visualization types built from additional trajectory data.

Query structures are constructed through the integration of spatio-temporal constraints where travel mode and altitude serving as core analytical dimensions (see Figure 6). This approach enables the creation of multiple query scenarios. Specifically, these scenarios support the aggregation of statistical data regarding user distribution across travel modes (e.g., walking, vehicle transportation), thereby enabling comparative visualizations such as bar charts and pie charts. Additionally, the fusion of trajectory metadata and sensor data, achieved through JOIN operations, enables the generation of line graphs that depict variations in altitude. Our current implementation supports three basic chart types: bar charts, line charts, and pie charts. The syntax specification is extensible to more complex visualization types, including heatmaps (e.g., travel mode-based population density) and scatter plots (e.g., location distribution).

### A.3 Synthesizing SQL from TVL

TVL	Synthesized SQL
<p><b>Visualize map</b>  <b>Area</b> Miyun District, Beijing  <b>ST</b> 2010-03-22 09:00:05  <b>ET</b> 2012-05-04 21:01:46</p> <pre>SELECT T1.traj_id, latitude, longitude, datetime FROM traj_data AS T1 JOIN add_traj_data AS T2 ON T1.traj_id = T2.traj_id WHERE user_id = 128 ORDER BY T1.traj_id, datetime</pre>	<pre>SELECT T1.traj_id, latitude, longitude, datetime FROM traj_data AS T1 JOIN add_traj_data AS T2 ON T1.traj_id = T2.traj_id WHERE ST_Within(ST_GeomFromText('POINT('    longitude    ' '    latitude    ')', 4326), (SELECT geom FROM boundaries WHERE city='Beijing' AND name='Miyun District'))='true' AND datetime BETWEEN '2010-03-22 09:00:05' AND '2012-05-04 21:01:46' AND user_id = 128 ORDER BY T1.traj_id, datetime</pre>

Figure 7: An example of Synthesizing SQL based on TVL.

Given the TVL specification in Figure 1, the system achieves translation to SQL by parsing the logical structure inherent in TVL. During this conversion, spatio-temporal constraints declared within the TVL are dynamically mapped to the WHERE clause of the resulting SQL query, specifically encompassing the core parameters: Area, ST (Start Time), and ET (End Time). For instance, when TVL specifies that the value of Area is "Miyun District, Beijing", ST is "2010-03-22 09:00:00", ET is "2012-05-04 21:01:00", and the basic SQL structure is "SELECT user\_id, traj\_id, latitude, longitude, datetime FROM traj\_data ORDER BY user\_id, traj\_id, datetime". Using these parameters, the system is able to dynamically generate the SQL required to query the data, as shown in Figure 7.

### A.4 Prompts for Generating NLQs

<p><b>Prompt for generating normal data</b></p> <p>Generate a natural language query for this TVL. The natural language needs to be fluent and consistent with the real world and needs to contain all the TVL information accurately.  TVL: {tv1}  Natural Language Query:</p>	<p><b>TVL:</b>  Visualize map  Area Miyun District, Beijing  ST 2010-03-22 09:00:05  ET 2012-05-04 21:01:46  SELECT T1.traj_id, latitude, longitude, datetime  FROM traj_data AS T1 JOIN add_traj_data AS T2 ON T1.traj_id = T2.traj_id WHERE user_id = 128 ORDER BY T1.traj_id, datetime</p> <p><b>NLQ1:</b>  Could you please visualize the map for the area Miyun District, Beijing from 2010-03-22 09:00:05 to 2012-05-04 21:01:46, showing the traj_id, latitude, longitude, and datetime for user 128?</p> <p><b>NLQ2:</b>  Could you show me a map of user 128 in the <i>Miyun area of Beijing</i>, focusing on the data from 2010-03-22 09:00:05 to 2012-05-04 21:01:46? I would like to see the trajectory information, including the trajectory ID, latitude, longitude, and the corresponding date and time.</p> <p><b>NLQ3:</b>  Please create a visualization of the map for the Miyun District in Beijing, focusing on the data collected <i>between the 22nd of March, 2010, at precisely 9:00 AM and 4th of May, 2012, at exactly 9:01 PM</i>. I would like to see the trajectory ID, latitude, longitude, and the date and time of the data points for user 128.</p>
<p><b>Prompt for different descriptions of area</b></p> <p>Generate a natural language query for this TVL. The natural language needs to be fluent and consistent with the real world and needs to contain all the TVL information accurately. Please describe the place name differently from the TVL, but make sure that they still represent the same place name.  TVL: {tv1}  Natural Language Query:</p>	
<p><b>Prompt for different descriptions of time</b></p> <p>Generate natural language query for this TVL. Natural language must be fluent and consistent with the real world and needs to accurately contain all the TVL information. Please describe the time in a different way than the TVL, but make sure they still represent the same time.  TVL: {tv1}  Natural Language Query:</p>	

Figure 8: The prompts for generating NLQs.

We designed prompt templates for LLM. These templates were categorized into three different types: (i) basic data generation: requiring that NLQs maintain semantic accuracy; (ii) diversification of area descriptions: including synonymous substitution of geographic names with enforced consistency of spatial references; and (iii) diversification of temporal descriptions: transforming standard time formats into natural language expressions, preserving the equivalence of the specified time ranges. Through this prompting strategy, the LLM generated three semantically consistent but differently formulated NLQs, as shown in Figure 8.

## A.5 Prompts for Correcting NLQs

### Prompt for correcting semantic redundancy

There is a problem with the description of the NLQ in the example data, the generated description contains information that is not relevant to the TVL.

## Given the NLQ in the example, perform the following actions:

1. Please examine the original NLQ carefully.
2. Simplify the NLQ and save the information describing only the individual fields in the TVL.
3. Correct it, and then regenerate a new NLQ to ensure that the information described is not redundant

## Example:

{relevant\_data}

## Note:

The answer just outputs each NLQ without additional text!

### Prompt for correcting information missing

There is a problem with the description of the NLQ in the example data, the description information generated based on the TVL is incomplete with missing information.

## Given the NLQ in the example, perform the following actions:

1. Regenerate a new NLQ based on the original NLQ.
2. Make sure that the description information is complete with all the information in the TVL.

## Example:

{relevant\_data}

## Note:

The answer just outputs each NLQ without additional text!

### Prompt for correcting information error

There is a problem with the description of the NLQ in the example data, the generated description information is inconsistent with the TVL in fields such as time, area, and SQL.

## Given the NLQ in the example, perform the following actions:

1. Examine the original NLQ carefully, find the inconsistent description and fix it.
2. Regenerate a new NLQ to ensure that the information in the description is consistent with the information in the TVL.

## Example:

{relevant\_data}

## Note:

The answer just outputs each NLQ without additional text!

Figure 9: The prompts for correcting NLQs.

## B More Experimental Setup

### B.1 Baselines

To comprehensively evaluate LLMs on the TrajVL dataset, we used a series of prompting strategies (few-shot learning) and RAG techniques. The model configurations are as follows:

- **Few-shot LLM:** The few-shot prompting is a core mechanism in In-Context Learning, using a limited set of examples to guide LLMs in performing tasks within specialized domains.
- **RAG for LLM:** Retrieval Augmented Generation (RAG) proposes an alternative methodological paradigm for LLM downstream task support. Unlike direct few-shot prompting, RAG dynamically retrieves the most contextually relevant examples from a curated knowledge base based on the model’s inputs. This process enriches the context available for LLM, thus reducing hallucination risks due to insufficient or ambiguous input data.
- **Llama3-8b:** Llama3-8b, an 8-billion-parameter open-weight language model developed by Meta, is optimized for high efficiency while maintaining robust performance across diverse NLP tasks. Pretrained on a large-scale multilingual corpus, it demonstrates strong reasoning and text-generation capabilities, positioning it as a versatile choice for applications requiring a balance between model size and inference speed.
- **Qwen2.5-7b:** Qwen2.5-7b, a 7-billion-parameter large language model developed by Alibaba Group, is engineered to deliver competitive performance in both general and domain-specific tasks. Trained on diverse multilingual and multimodal corpora, it excels in natural language understanding, generation, and code-related tasks, while maintaining computational efficiency.
- **DeepSeek-llm-7b:** DeepSeek-llm-7b, a 7-billion-parameter LLM developed by DeepSeek, is designed to provide a strong balance between performance and computational efficiency. Pretrained on extensive text and code corpora, it exhibits competitive capabilities in various natural language understanding and generation tasks, making it a suitable option for applications where resource constraints are a consideration.
- **GPT-4o-mini:** GPT-4o-mini, a smaller version in OpenAI’s GPT-4o series, leverages advanced architectures and training methodologies for strong performance on diverse NLP tasks. Designed for efficiency and responsiveness, it offers a balance between high-quality generation and reduced latency, making it suitable for applications requiring both sophisticated language understanding and rapid response times.

### B.2 Metrics

We use the same metrics as NVBench, including Vis Accuracy, Axis Accuracy, and Data Accuracy, to assess LLM performance in TVL generation. Since spatio-temporal information is important for trajectory data, SQL statements for trajectory queries are synthesized based on area, time and basic SQL query structure. Consequently, Data Accuracy is decomposed into Area Accuracy, Time Accuracy, SQL Accuracy and TVL Accuracy.

The evaluation metrics are formally defined as follows:

- **Vis Accuracy (Vis.Acc):** This metric evaluates the accuracy of the Visualize component of the TVL generated by the model, measuring the model’s ability to identify the type of visualization. It is calculated as:

$$Acc_{type} = \frac{N_{type}}{N}$$

Where  $N_{type}$  represents the count of exact match visualization types,  $N$  represents the total number of visualization types in the test set.

- **Axis Accuracy (Axis.Acc):** This metric evaluates the performance of the model in recognizing vis components. For map visualizations, it evaluates the accuracy of the Area generated by the model, since proper visualization requires centering of the specified area for map visualizations. For the x-axis and y-axis components of other types of visualizations such as bar, line, pie, etc., we measure the Select component of the vis query. It is calculated as:

$$Acc_{comp} = \frac{N_{comp}}{N}$$

Where  $N_{comp}$  represents the count of exact matches to the Area or Select component,  $N$  represents the total number of queries in the test set.

- **Area Accuracy (Area.Acc):** This metric evaluates the accuracy of the Area component of the TVLs generated by the model to reveal the model's performance in recognizing geographical area names. It is calculated as:

$$Acc_{area} = \frac{N_{area}}{N}$$

Where  $N_{area}$  represents the count of exact matching Area components,  $N$  represents the total number of queries in the test set.

- **Time Accuracy (Time.Acc):** This metric evaluates the accuracy of the Time component of the TVLs generated by the model to reveal the model's performance in recognizing temporal information. It is calculated as:

$$Acc_{time} = \frac{N_{time}}{N}$$

Where  $N_{time}$  represents the count of exact matching Time components,  $N$  represents the total number of queries in the test set.

- **SQL Accuracy (SQL.Acc):** This metric evaluates the accuracy of the model in generating critical SQL by parsing and comparing SQL query structures in TVL. Specifically, it eliminates interference from syntactically equivalent but ordering differences through normalization (e.g., alphabetizing logical conditions in WHERE clauses), and recursively compares SQL structures through parse trees. It is calculated as:

$$Acc_{sql} = \frac{N_{sql}}{N}$$

Where  $N_{sql}$  represents the count of exact matching SQL queries,  $N$  represents the total number of SQL queries in the test set.

- **TVL Accuracy (TVL.Acc):** This metric evaluates the accuracy of the model in generating a complete TVL. Based on the structure of the TVL, a model is considered to be able to generate the TVL correctly when it correctly generates Visualize, Area, Time and SQL. It is calculated as:

$$Acc_{tv} = \frac{N_{tv}}{N}$$

Where  $N_{tv}$  represents the count of exact match TVLs,  $N$  represents the total number of TVLs in the test set.

### B.3 Implementation Details.

Our experiments used three open-source LLMs (Llama3-8b, Qwen2.5-7b, DeepSeek-llm-7b) and one closed-source LLM (GPT-4o-mini). We conducted experiments in both the baseline configuration and the RAG-enhanced configuration. In the baseline configuration, the LLM was used directly. In the RAG-enhanced configuration, a vector library constructed using the *all-mpnet-base-v2* model was used to provide context prompts. During the inference process, the top-k most similar samples are retrieved from the vector library, where k ranged from 1 to 3. The temperature parameter for all LLMs was set to 0.1 and the max\_length was set to 2048 tokens.

### B.4 Prompt for Experiment

```
You are an expert in Natural Language Visualization (NL2VIS).
Your task is to parse an input Natural Language Question and translate it into a structured TVL
format.

## Database Schema:
- traj_data (id, traj_id, latitude, longitude, datetime)
- add_traj_data (id, traj_id, altitude, travel_mode, user_id)

## Instructions:
1. Strict Output Format: Your response must contain only one TVL query—no explanations,
preambles, additional text.
2. Parsing Requirements:
- Identify the geographic area mentioned.
- Extract filtering conditions (e.g., altitude range, time constraints).
- Select relevant fields from the appropriate tables.

## Example:
{relevant_data}

## Now, Process this Input:
### Input (NLQ):
NLQ: {query_text}
### Output (TVL):
Your response must strictly follow this format and only return the TVL query:
TVL: Visualize [visualize] Area [area] ST [st] ET [et] [sql]
```

Figure 10: The prompt for LLMs to generate TVLs in experiment.

## C More Experimental Details

### C.1 Performance of Few-shot LLMs on Dataset

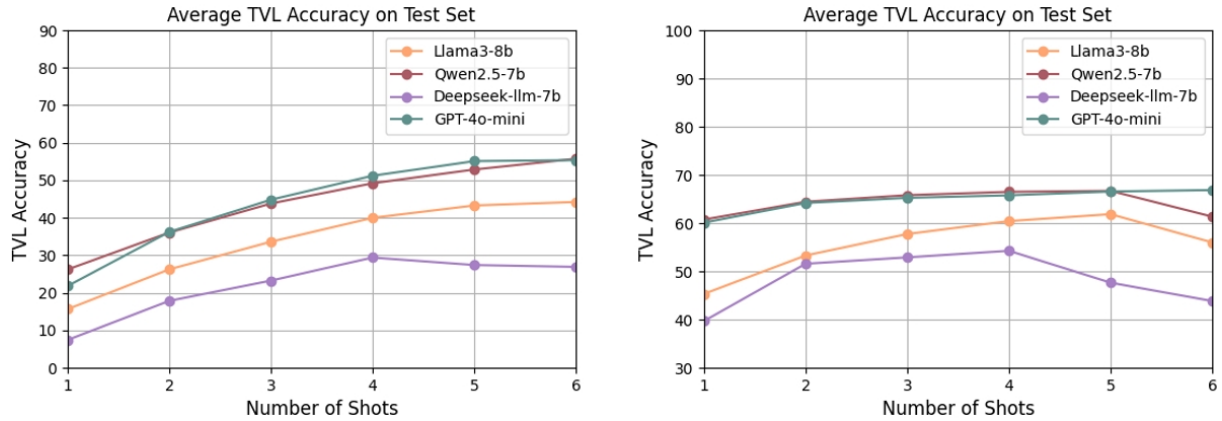


Figure 11: Average performance of LLMs on three test sets.

We systematically evaluated the impact of few-shot learning on model performance by experimentally comparing the performance of Llama3-8b, Qwen2.5-7b, DeepSeek-llm-7b, and GPT-4o-mini under the baseline configuration and RAG enhancement, as shown in Figure 10. The experimental results show that the average accuracy of LLMs under the base setting shows an increasing trend for both 1-5 shot scenarios. The performance of DeepSeek-llm-7b starts to decrease at 4-shot. The average accuracy of RAG-enhanced LLMs shows an increasing trend across 1-5 shot scenarios. The performance of DeepSeek-llm-7b starts to decrease at 4-shot. The performance of Llama3-8b and Qwen2.5-7b starts to decrease at 5-shot. Consequently, we analyzed in detail the experimental results for the sample scenario with the best performance of LLMs for both experimental settings in Section 5.

## C.2 One-shot LLMs’ Performance Comparison

Test Set	Model	Vis.Acc	Axis.Acc	Data.Acc			
				Area	Time	SQL	TVL
Normal	DeepSeek-llm-7b	96.10	49.77	42.02	51.19	17.79	8.92
	Llama3-8b	99.44	67.76	67.11	66.95	24.73	20.27
	Qwen2.5-7b	100.0	77.70	75.57	81.65	35.48	30.82
	GPT-4o-mini	79.02	75.82	78.16	66.19	29.19	23.01
Area	DeepSeek-llm-7b	100.0	46.43	28.94	42.02	14.34	5.27
	Llama3-8b	99.34	56.41	44.70	66.09	21.79	12.77
	Qwen2.5-7b	99.95	67.56	56.72	89.15	34.77	22.71
	GPT-4o-mini	92.85	71.41	65.99	70.05	36.19	18.80
Time	DeepSeek-llm-7b	99.95	52.51	36.09	34.21	16.22	8.01
	Llama3-8b	99.80	66.70	61.43	59.66	19.46	13.89
	Qwen2.5-7b	100.0	77.04	72.93	73.75	72.74	25.09
	GPT-4o-mini	90.47	80.54	82.32	54.74	35.28	20.58

Table 5: Comparison of performance for each LLM on TrajVL.

Test Set	Model	Vis.Acc	Axis.Acc	Data.Acc			
				Area	Time	SQL	TVL
Normal	DeepSeek-llm-7b	100.0	82.01	70.25	88.55	57.27	46.27
	Llama3-8b	99.29	82.26	76.28	84.64	61.33	51.39
	Qwen2.5-7b	100.0	96.76	95.13	98.07	73.59	70.86
	GPT-4o-mini	96.05	94.88	94.27	95.84	70.45	68.98
Area	DeepSeek-llm-7b	99.75	77.90	61.23	87.58	46.68	30.50
	Llama3-8b	98.94	72.17	57.02	85.71	54.28	36.54
	Qwen2.5-7b	99.75	81.65	70.45	98.68	66.35	48.61
	GPT-4o-mini	98.68	82.41	72.53	94.98	66.65	47.80
Time	DeepSeek-llm-7b	99.90	89.25	77.60	79.07	53.93	42.32
	Llama3-8b	99.09	84.90	76.23	83.73	59.45	48.05
	Qwen2.5-7b	99.95	96.86	94.58	94.48	70.70	62.75
	GPT-4o-mini	98.94	95.95	94.58	94.08	70.25	63.56

Table 6: Comparison of performance for each RAG-enhanced LLM on TrajVL.

Multiple LLMs were evaluated on three test sets, including GPT-4o-mini, Llama3-8b, DeepSeek-llm-7b, and Qwen2.5-7b. Table 5 and Table 6 summarize the performance of these LLMs in both baseline and RAG-enhanced configurations under the 1-shot setting. The results indicate that RAG yielded a substantial improvement in TVL accuracy of these models on the three test sets. While RAG-enhanced 1-shot learning approached the performance of multi-shot learning on basic tasks, a performance gap remained in complex scenarios. In particular, in the Area test set, the TVL accuracy in one-shot scenarios is significantly lower than that of few-shot. In normal scenarios, RAG significantly improved semantic parsing and TVL generation capabilities, with DeepSeek-llm-7b showing a notable increase in TVL and SQL generation accuracy. However, the benefits of RAG were limited in complex scenarios. For instance, the TVL accuracy of Qwen2.5-7b in the Area test set increased only from 22.71% to 48.61%. This increase, which is much lower than the percentage improvement in normal scenarios, indicates the complex area descriptions that pose a challenge to the models.

We also observed that In-Context Learning (ICL) effectively mitigates performance deficits in specialized domains, although the number of contextual examples significantly influenced model performance. Specifically, in the three experiments detailed in Section 5, the top-performing GPT-4o-mini achieved TVL accuracies of 64.67%, 47.74%, and 56.66% across the three test sets, respectively, demonstrating a substantial improvement over the 1-shot configurations. While RAG-enhanced LLMs in a 1-shot setting did not surpass the best-performing few-shot setups, their performance remained closely competitive, highlighting the importance of external knowledge retrieval through RAG.